American Mineralogist, Volume 84, pages 1–14, 1999

Relating formulations of the thermodynamics of mineral solid solutions: Activity modeling of pyroxenes, amphiboles, and micas

ROGER POWELL[1,*] AND TIM HOLLAND[2]

[1]School of Earth Sciences, University of Melbourne, Parkville, Victoria 3052 Australia
[2]Department of Earth Sciences, University of Cambridge, Cambridge, U.K.

ABSTRACT

In a thermodynamic description of a mineral solid solution, it is customary to select a minimal group of end-members that constitutes an independent set, and yet in practical calculations it commonly occurs that a different independent set or subset is required. Given the simplification of the symmetric formalism, it is straightforward to derive the enthalpies of formation of dependent end-members as well as the interaction energies between the end-members in the new independent set, in terms of those in the original set. For example, a simplified ternary solid solution of Fe-free Ca-amphiboles might be described with independent end-members tremolite, tschermakite, and pargasite, and yet some calculations may require the use of end-members such as edenite or hornblende. Not only are their end-member properties dependent on those of the first three, but the mixing properties of any of the binary joins involving edenite or hornblende are dependent on those in the original independent set. Examples drawn from pyroxenes, amphiboles, and biotite micas show that such dependencies may prove invaluable in using experimental information or heuristics to help constrain the mixing properties of complex solid solutions. In particular, it is found that in non-ideal solid solutions that involve Fe and Mg distributed over two or more non-equivalent sites, equipartition of Fe and Mg implies extreme restrictions on the ratios of the interaction parameters and the magnitude of the Fe-Mg exchange energy. The thermodynamics can only be formulated generally and consistently when Fe-Mg ordering is explicitly included, and this is done most simply via ordered Fe-Mg end-members.

INTRODUCTION

Expressing the thermodynamics of mixing in mineral solid solutions generally involves choosing a convenient set of independent end-members for the problem at hand. An example at the simplest level is that of tschermakitic amphiboles in the CaO-MgO-Al_2O_3-SiO_2-H_2O system, in which the choice of whether to use tschermakite [ts, $Ca_2Mg_3Al_4Si_6O_{22}(OH)_2$] or hornblende [hb, $Ca_2Mg_4Al_2Si_7O_{22}(OH)_2$] as the aluminous end-member is arbitrary. If thermodynamic data exist for the solid solution in terms of tremolite-tschermakite, it is straightforward to generate thermodynamic data for hornblende and, if the system is ideal, the relationships are particularly simple. In this case, the Gibbs energy of hornblende is $G_{hb} = ½ (G_{ts} + G_{tr}) - TS^{conf}_{hb}$, stemming from the reaction relation 2hb = ts + tr, where tr is tremolite [$Ca_2Mg_5Si_8O_{22}(OH)_2$], with addition of the configurational entropy present in hornblende through mixing of Al-Mg on the M2 site and Al-Si on the T1 sites. However, if the join tremolite-tschermakite is non-ideal, say, regular with interaction energy $W_{tr\text{-}ts}$, then a re-formatting of the thermodynamics in terms of tremolite-hornblende requires further considerations, best illustrated in Figure 1. The enthalpy of the hornblende end-member is larger than the average of tremolite + tschermakite because of the non-ideal enthalpy of mixing ($x_{tr}x_{ts}\ W_{tr\text{-}ts} = ¼W_{tr\text{-}ts}$). Also, the magnitude of the mixing enthalpy between tremolite and hornblende is smaller than between tremolite and tschermakite ($W_{tr\text{-}hb} = ¼W_{tr\text{-}ts}$). In a binary these relationships are easy to derive, but for complex systems a more systematic approach is required. Such an approach for deriving the thermodynamic relationships for dependent end-members is outlined here.

The purpose of this paper is to investigate the macroscopic consequences of considering different independent sets of end-members when non-ideal mixing is involved. Examples will be used, and the reader is urged to view them primarily as vehicles to illustrate the uses and consequences of changing independent sets of end-members. While care has been taken to make these examples realistic and useful, it must be stressed that presentation of optimal activity models is not their intended use. In what follows, the thermodynamics of non-ideal mixing are taken, for simplicity of argument, to be macroscopic regular between all pairs of end-members. In the symmetric formalism for multi-component multi-site phases (Powell and Holland 1993; Holland and Powell 1996a, 1996b),

* E-mail: tjbh@esc.cam.ac.uk

0003–004X/99/0102–0001$05.00

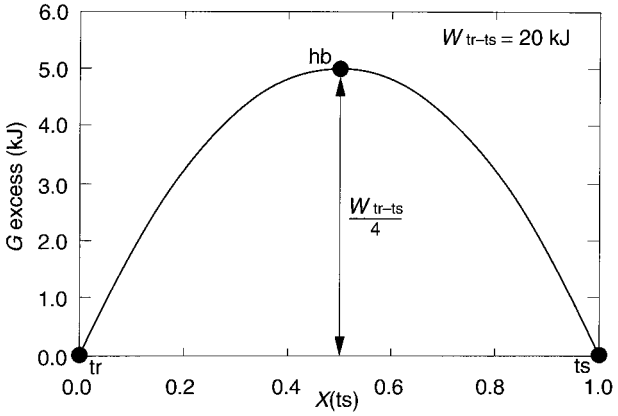

FIGURE 1. Excess free energy of amphiboles in the system tremolite-hornblende-tschermakite (tr, hb, and ts, respectively). The hb end-member has a higher Gibbs energy than a linear combination of tr and ts by $¼W_{tr\text{-}ts}$. The regular solution parameter for the binaries tr-hb and hb-ts are ¼ of that for the binary tr-ts.

the non-ideal contribution to the Gibbs energy of mixing can be written as

$$G^{ex} = \sum_{i=1}^{n-1} \sum_{j=i+1}^{n} p_i p_j W_{ij} \tag{1}$$

In this expression, which has the same form as that introduced by Benedict et al. (1945), p_i and p_j are the proportions of end-members i and j in an independent set of end-members, and the W_{ij} are macroscopic interaction energies. These interaction energies could, but need not, be regarded as linear combinations of the microscopic same-site and cross-site interaction energies. The $p_i p_j W_{ij}$ terms are simply symmetric expressions for non-ideality, whatever their origin, of the same algebraic form as regular-type interactions. The symmetric formalism is quadratic in composition and, for the purposes of this paper, all terms cubic in composition (and hence any ternary interaction parameters) will not be considered.

The number of end-members in the independent set is determined by the number of components needed to represent the macroscopic composition of the phase, augmented by the number of order-disorder parameters needed to represent the microscopic arrangement of the atoms. So, for example, in representing (stoichiometric) orthopyroxene in the system, FeO-MgO-SiO_2, with Fe-Mg order-disorder on the Ml and M2 sites, there are two components (say $Fe_2Si_2O_6$ and $Mg_2Si_2O_6$) and one order parameter (say $x_{Fe}^{M2} - x_{Fe}^{M1}$), giving an independent set with three end-members (say fs, $Fe_2Si_2O_6$, en, $Mg_2Si_2O_6$ and the ordered end-member, fm, $FeMgSi_2O_6$, with Fe on M2 and Mg on M1). The independent set of end-members used in the symmetric formalism is the choice of the user, the underlying thermodynamics being equivalent in each case. So, in the orthopyroxene example, the anti-ordered end-member $MgFeSi_2O_6$ could be used. However, because the underlying thermodynamics are the same, the formulations with different independent sets of end-members must involve equivalencies among the p terms and more particularly among the W terms. In the context of the thermodynamic dataset of Holland and Powell (1990), in which ideal mixing on sites was used for the majority of phases, such equivalencies were not needed: The thermodynamic data for dependent end-members were found by linear combination of the data for end-members in the dataset. However, with increasing need to use non-ideal models, with data now available to constrain non-ideality, such a simple approach is no longer sufficient.

Knowing the equivalences among formulations of the thermodynamics of a mineral is much more than a matter of having a complete thermodynamic description, it is a powerful tool in calibrating the thermodynamic description itself, in combination with heuristics concerning interaction energies that are likely to be similar.

DERIVATION

The starting point is to write the Gibbs energy of a mineral, G, as the sum of the non-configurational (G^*) and the ideal configurational ($-TS_c$) parts, as $G = G^* - TS_c$, with

$$G^* = \sum_{i=1}^{n-1} p_i G_i = \sum_{i=1}^{n-1} \sum_{j=i+1}^{n} p_i p_j W_{ij} \tag{2}$$

in which G_i is the Gibbs energy of end-member i, and n being the number of end-members in the independent set. The configurational part of the Gibbs energy is found from ideal mixing on sites and is not discussed further. It is convenient to write the p_k as a (column) vector, $\boldsymbol{p}$, the Gibbs energies of the end-members as a vector, $\boldsymbol{g}$, and the W's as a strictly upper trangular matrix, $\mathbf{W}$:

$$\boldsymbol{W} = \begin{pmatrix} 0 & W_{12} & W_{13} & W_{14} & \cdots & W_{1n} \\ 0 & 0 & W_{23} & W_{24} & \cdots & W_{2n} \\ 0 & 0 & 0 & W_{34} & \cdots & W_{3n} \\ 0 & 0 & 0 & 0 & \cdots & W_{4n} \\ \vdots & \vdots & \vdots & \vdots & \ddots & \vdots \\ 0 & 0 & 0 & 0 & 0 & 0 \end{pmatrix} \tag{3}$$

Strictly upper trangular matrices have zeroes along the main diagonal, as well as beneath it. With this G^* Equation 2 can be written as the matrix equation

$$G^* = \boldsymbol{p}^T\boldsymbol{g} + \boldsymbol{p}^T\boldsymbol{W}\boldsymbol{p} \tag{4}$$

The proportions of the end-members in one independent set, $\boldsymbol{p}$, can be converted to the proportions in another, $\boldsymbol{p'}$, with a linear transform, represented by a matrix, $\boldsymbol{A}$

$$\boldsymbol{p} = \boldsymbol{A}\boldsymbol{p'} \text{ and } \boldsymbol{p'} = \boldsymbol{A}^{-1}\boldsymbol{p} \tag{5}$$

in which $\boldsymbol{A}^{-1}$ is the inverse of $\boldsymbol{A}$. The transform matrix is calculated from the matrix of the mineral compositions, with each row of this composition matrix being the composition of an end-member in the independent set. If $\boldsymbol{C}$ is the composition matrix for the initial set, and $\boldsymbol{C'}$ the

TABLE 1A. Mathematica function, *depem,* to perform transformation

```
transform[c:{{_?NumberQ...}...},cp:{{_?NumberQ...}...},
        name_List, namep_List] :=

 Module[{n,m,a,pos,A,w,q,wp,h,hp,z},

  {n,m} = Dimensions[c];
  a = Map[NullSpace[Transpose[Join[c,{-#}]]]&,cp];

  If[Dimensions[a] != {n,1,n+1}, Print["not soluble"]; "not OK",
    A = Transpose[Map[Drop[#[[1]],-1]/#[[1,-1]]&,a]];
    w = Table[If[i<j, StringJoin["w[",ToString[name[[i]]],",",
                                 ToString[name ob[[j]]],"]"],0],
              {i,n},{j,n}];

    q = Transpose[A].w.A;
    q += Array[(k = #; Array[If[#==k, 0, -q[[k,k]]]&, n])&, n];

    wp = Table[If[i<j, Simplify[q[[i,j]]+q[[j,i]]],0],{i,n},{j,n}];

    Map[(i = #; Map[Print["w'[",namep[[i]],",",namep[[#]],"]= ",
                    wp[[i,#]]]&, Range[i+1,n]])&, Range[n-1]];
    Print["  "];

    h = Map[StringJoin["g[",ToString[name[[#]]],"]"]&, Range[n]];
    hp = Simplify[Transpose[A].h + Array[q[[#,#]]&,n]];
    Map[Print["g'[",namep[[#]],"]= ",hp[[#]]]&, Range[n]]; "OK"]]/;
        Length[name] == Length[namep] && Dimensions[c] == Dimensions[cp];
```

composition matrix corresponding to $\boldsymbol{p'}$, then $\boldsymbol{A}$ can be found from $\boldsymbol{C'} = \boldsymbol{A}^{\mathrm{T}}\boldsymbol{C}$, which $\boldsymbol{A}^{\mathrm{T}}$ is the transpose of $\boldsymbol{A}$.

In the different independent set, G^* is written in terms of $\boldsymbol{p'}$, and the corresponding interaction energies, $\boldsymbol{W'}$, and Gibbs energies, $\boldsymbol{g'}$, in an equivalent expression to (4)

$$G^* = \boldsymbol{p'}^{\mathrm{T}}\boldsymbol{g'} + \mathbf{p'}^{\mathrm{T}}\boldsymbol{W'}\boldsymbol{p'} \tag{6}$$

Given that the right hand sides of Equations 4 and 6 are identically equal, these equations allow $\boldsymbol{g}$ and $\boldsymbol{W}$ to be related to $\boldsymbol{g'}$ and $\boldsymbol{W'}$. First, combining Equations 5 with 4 gives

$$\begin{aligned} G^* &= \boldsymbol{p'}^{\mathrm{T}}\boldsymbol{A}^{\mathrm{T}}\boldsymbol{g} + \boldsymbol{p'}^{\mathrm{T}}\boldsymbol{A}^{\mathrm{T}}\boldsymbol{W'}\boldsymbol{A}\boldsymbol{p'} \\ &= \boldsymbol{p'}^{\mathrm{T}}\boldsymbol{A}^{\mathrm{T}}\boldsymbol{g} + \boldsymbol{p'}^{\mathrm{T}}\boldsymbol{Q}\boldsymbol{p'} \end{aligned} \tag{7}$$

in which $\boldsymbol{Q} = \boldsymbol{A}^{\mathrm{T}}\boldsymbol{W}\boldsymbol{A}$. Comparing Equations 7 with 4, $\boldsymbol{Q}$ will not in general be strictly upper triangular, as $\boldsymbol{W}$ is in Equation 4, and as it needs to be, so the requirement is to convert $\boldsymbol{Q}$ to the form of Equation 3. Some terms will end up not being able to be included in $\boldsymbol{W'}$, and these are transferred to $\boldsymbol{g'}$. To do the conversion, $\boldsymbol{Q}$ is written as $\boldsymbol{Q}_1 + \boldsymbol{Q}_2 + \boldsymbol{Q}_3$, in which $\boldsymbol{Q}_1$ is that part of $\boldsymbol{Q}$ below the diagonal with zeroes on the diagonal and above; $\boldsymbol{Q}_2$ is that part $\boldsymbol{Q}$ above the diagonal with zeroes on the diagonal and below; and $\boldsymbol{Q}_3$ is a diagonal matrix containing the diagonal elements of $\boldsymbol{Q}$. The first contributions to $\boldsymbol{W'}$ come from $\boldsymbol{Q}_1^{\mathrm{T}}$ and $\boldsymbol{Q}_2$. Transposing turns the strictly lower triangular matrix $\boldsymbol{Q}_2$ into a strictly upper triangular one. Zeroing $\boldsymbol{Q}_3$ is done by noting that the terms in Equation 7 from $\boldsymbol{Q}_3$ have the form $p_k^2\boldsymbol{Q}_{3k}$. These terms can be written as $p_k(1 - \Sigma_{j \neq k} p_j)\, \boldsymbol{Q}_{3k}$. As a consequence the diagonal elements of $\boldsymbol{Q}_3$ contribute to both $\boldsymbol{g'}$ and $\boldsymbol{W'}$. Writing $p_k(1 - \Sigma_{j \neq k} p_j)\, \boldsymbol{Q}_{3k} = p_k\boldsymbol{Q}_{3k} - \Sigma_{j \neq k} p_j p_k \boldsymbol{Q}_{3k}$, the first part has $\boldsymbol{Q}_{3k}$ becoming the kth element of a vector $\boldsymbol{q}$, that contributes to $\boldsymbol{g'}$ in the form $\boldsymbol{p'}^{\mathrm{T}}\boldsymbol{q}$. The second part has $\boldsymbol{Q}_{3k}$ being entered as elements in the kth row and the kth column of a strictly upper triangular matrix, $\boldsymbol{Q'}_3$, that contributes to $\boldsymbol{W'}$ in the form $\boldsymbol{p'}^{\mathrm{T}}\, \boldsymbol{Q'}_3\, \boldsymbol{p'}$. Thus Equation 7 becomes

$$\begin{aligned} G^* &= \boldsymbol{p'}^{\mathrm{T}}(\boldsymbol{A}^{\mathrm{T}}\boldsymbol{g} + \boldsymbol{q}) + \boldsymbol{p'}^{\mathrm{T}}(\boldsymbol{Q}_1^{\mathrm{T}} + \boldsymbol{Q}_2 + \boldsymbol{Q}'_3)\boldsymbol{p'} \\ &= \boldsymbol{p'}^{\mathrm{T}}\boldsymbol{g'} + \boldsymbol{p'}^{\mathrm{T}}\boldsymbol{W'}\boldsymbol{p'} \end{aligned} \tag{8}$$

as required.

A *Mathematica* function, *depem*, is provided in Table 1 that implements this approach; it was used to produce all of the transformations presented here. It is also available with all of the examples on the web at URL http://rubens.unimelb.edu.au/~rpowell.

EXAMPLES

Orthopyroxene

The first example concerns orthopyroxene in the system FeO-MgO-Al_2O_3-SiO_2, with Fe-Mg order-disorder between the Ml and M2 sites, and octahedral Al is here assumed to be located only on M1 (Fig. 2). The composition matrix of an independent set involving enstatite (en; $MgMgSi_2O_6$), ferrosilite (fs; $FeFeSi_2O_6$), Mg-Tschermak's pyroxene (mgts; $MgAlAlSiO_6$), and Fe-Mg-ordered pyroxene (fm; $FeMgSi_2O_6$) is

$$\boldsymbol{C} = \begin{array}{c} \\ \text{en} \\ \text{fs} \\ \text{mgts} \\ \text{fm} \end{array} \begin{array}{c} \begin{array}{ccccccc} n_{\mathrm{Fe}}^{\mathrm{M2}} & n_{\mathrm{Mg}}^{\mathrm{M2}} & n_{\mathrm{Fe}}^{\mathrm{M1}} & n_{\mathrm{Mg}}^{\mathrm{M1}} & n_{\mathrm{Al}}^{\mathrm{M1}} & n_{\mathrm{Al}}^{\mathrm{T}} & n_{\mathrm{Si}}^{\mathrm{T}} \end{array} \\ \begin{pmatrix} 0 & 1 & 0 & 1 & 0 & 0 & 2 \\ 1 & 0 & 1 & 0 & 0 & 0 & 2 \\ 0 & 1 & 0 & 0 & 1 & 1 & 1 \\ 1 & 0 & 0 & 1 & 0 & 0 & 2 \end{pmatrix} \end{array} \tag{9}$$

in which the n_i^j denote the number of atoms of i on the

TABLE 1B. Function, *depem,* used to perform transformation for the orthopyroxene example

```
Input:

  name = {"en","fs","mgts","fm"};

  c = {{0, 1, 0, 1, 0,   0, 2},
       {1, 0, 1, 0, 0,   0, 2},
       {0, 1, 0, 0, 1,   1, 1},
       {1, 0, 0, 1, 0,   0, 2}};

  namep = {"en","fs","fets","fm"};

  cp = {{0, 1, 0, 1, 0,   0, 2},
        {1, 0, 1, 0, 0,   0, 2},
        {1, 0, 0, 0, 1,   1, 1,}
        {1, 0, 0, 1, 0,   0, 2}};

transform[c, cp, name, namep];

output:

  w'[en, fs] = w[en, fs]
  w'[en, fets] = 2 w[en, mgts] + 2 w[en, fm] − w[mgts, fm]
  w'[en, fm] = w[en, fm]
  w'[fs, fets] = −w[en, fs] + w[en, mgts] + w[en, fm] + w[fs, mgts] + w[fs, fm] − w[mgts, fm]
  w'[fs, fm] = w[fs, fm]
  w'[fets, fm] = w[en, mgts]

  g'[en] = g[en]
  g'[fs] = g[fs]
  g'[fets] = −g[en] + g[mgts] + g[o] − w[en, mgts] − w[en, fm] + w[mgts, fm]
  g'[o] = g[o]
```

site j. Using $\boldsymbol{C}$, the relationship between the proportions of the end-members in the independent set (p_{en}, p_{fs}, p_{mgts}, and p_{fm}) and the composition variables used to characterize the phase can be determined, as outlined in part a of Appendix 1. Here, choosing the composition variables to be

$$y = n^{M1}_{Al}, \qquad x_1 = \left(\frac{n^{M1}_{Fe}}{n^{M1}_{Fe} + n^{M1}_{Mg}}\right) \quad \text{and}$$

$$x_2 = \left(\frac{n^{M2}_{Fe}}{n^{M2}_{Fe} + n^{M2}_{Mg}}\right),$$

$$p_{en} = 1 - x_2 - y$$

$$p_{fs} = x_1(1 - y)$$

$$p_{mgts} = y$$

$$p_{fm} = x_2 - x_1(1 - y) \tag{10}$$

Considering the determination of equivalences in changing the independent set of end-members, one that could be addressed is the discovery of the consequences of a plausible assumption that $\boldsymbol{W}_{\text{en-mgts}} \approx \boldsymbol{W}_{\text{fs-fets}}$, in which fets is Fe-Tschermak's pyroxene ($FeAlAlSiO_6$). The idea here is that such an assumption, leading to equivalences between $\boldsymbol{W}$'s, makes the specification of the thermodynamics of orthopyroxene easier to achieve. Thus, although the original choice of an independent set is an appropriate one, looking at relationships between this set and one containing fets results in constraints among the $\boldsymbol{W}$'s in the original set. The new set will involve fets instead of mgts. Independent of the algebra in the previous section, the non-trivial relationship between the macroscopic $\boldsymbol{W}$'s in the two independent sets can be seen by looking at the equations for the macroscopic $\boldsymbol{W}$'s in terms of the microscopic contributions (assuming that these contributions are all of a configurational type). An example of these relationships for orthopyroxene is given in Appendix 2.

The composition matrix of the new independent set is

$$\boldsymbol{C}' = \begin{array}{c} \\ \text{en} \\ \text{fs} \\ \text{fets} \\ \text{fm} \end{array} \begin{array}{c} \begin{array}{ccccccc} n^{M2}_{Fe} & n^{M2}_{Mg} & n^{M1}_{Fe} & n^{M1}_{Mg} & n^{M1}_{Al} & n^{T}_{Al} & n^{T}_{Si} \end{array} \\ \begin{pmatrix} 0 & 1 & 0 & 1 & 0 & 0 & 2 \\ 1 & 0 & 1 & 0 & 0 & 0 & 2 \\ 1 & 0 & 0 & 0 & 1 & 1 & 1 \\ 1 & 0 & 0 & 1 & 0 & 0 & 2 \end{pmatrix} \end{array} \tag{11}$$

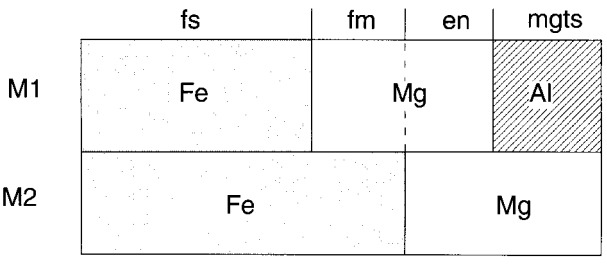

FIGURE 2. Block diagram showing site occupancy and proportion of end-members (fs, fm, en, and mgts) in FMAS orthopyroxenes.

Finding the transform matrix $\boldsymbol{A}$ so that $\boldsymbol{C}' - \boldsymbol{A}^{\mathrm{T}}\boldsymbol{C}$, is outlined in part b of Appendix 1. Then, using Equation 5

$$\boldsymbol{p}' = \begin{pmatrix} p'_{\mathrm{en}} \\ p'_{\mathrm{fs}} \\ p'_{\mathrm{fets}} \\ p'_{\mathrm{fm}} \end{pmatrix} = \boldsymbol{A}^{-1}\boldsymbol{p} = \begin{pmatrix} 1 & 0 & 1 & 0 \\ 0 & 1 & 0 & 0 \\ 0 & 0 & 1 & 0 \\ 0 & 0 & -1 & 1 \end{pmatrix} \cdot \begin{pmatrix} p_{\mathrm{en}} \\ p_{\mathrm{fs}} \\ p_{\mathrm{mgts}} \\ p_{\mathrm{fm}} \end{pmatrix}$$

$$= \begin{pmatrix} p_{\mathrm{en}} + p_{\mathrm{mgts}} \\ p_{\mathrm{fs}} \\ p_{\mathrm{mgts}} \\ -p_{\mathrm{mgts}} + p_{\mathrm{fm}} \end{pmatrix} \tag{12}$$

Note that the proportions of en and fm are different in the two independent sets.

With $\boldsymbol{A}$, the $\boldsymbol{W}$ equivalences can be established via Equations 7 and 8, as shown in part c of Appendix 1, or using the *Mathematica* function in Table 1. These equivalences can be represented using the matrix equation

$$\begin{pmatrix} W'_{\text{en-fs}} \\ W'_{\text{en-fets}} \\ W'_{\text{en-fm}} \\ W'_{\text{fs-fets}} \\ W'_{\text{fs-fm}} \\ W'_{\text{fets-fm}} \end{pmatrix} = \begin{array}{c} \begin{matrix} W_{\text{en-fs}} & W_{\text{en-mgts}} & W_{\text{en-fm}} & W_{\text{fs-mgts}} & W_{\text{fs-fm}} & W_{\text{mgts-fm}} \end{matrix} \\ \begin{pmatrix} 1 & 0 & 0 & 0 & 0 & 0 \\ 0 & 2 & 2 & 0 & 0 & -1 \\ 0 & 0 & 1 & 0 & 0 & 0 \\ -1 & 1 & 1 & 1 & 1 & -1 \\ 0 & 0 & 0 & 0 & 1 & 0 \\ 0 & 1 & 0 & 0 & 0 & 0 \end{pmatrix} \end{array} \cdot \begin{pmatrix} W_{\text{en-fs}} \\ W_{\text{en-mgts}} \\ W_{\text{en-fm}} \\ W_{\text{fs-mgts}} \\ W_{\text{fs-fm}} \\ W_{\text{mgts-fm}} \end{pmatrix} \tag{13}$$

or

$$\begin{aligned} W'_{\text{en-fs}} &= W_{\text{en-fs}} \\ W'_{\text{en-fets}} &= 2W_{\text{en-mgts}} + 2W_{\text{en-fm}} - W_{\text{mgts-fm}} \\ W'_{\text{en-fm}} &= W_{\text{en-fm}} \\ W'_{\text{fs-fets}} &= -W_{\text{en-fs}} + W_{\text{en-mgts}} + W_{\text{en-fm}} + W_{\text{fs-mgts}} + W_{\text{fs-fm}} \\ &\quad - W_{\text{mgts-fm}} \\ W'_{\text{fs-fm}} &= W_{\text{fs-fm}} \\ W'_{\text{fets-fm}} &= W_{\text{en-mgts}} \end{aligned} \tag{14}$$

Although some of the equivalences are obvious or intuitive (for example, the last one involves just MgAl mixing of M1), other involve more complex combinations. Also,

$$\begin{pmatrix} g'_{\mathrm{en}} \\ g'_{\mathrm{fs}} \\ g'_{\mathrm{fets}} \\ g'_{\mathrm{fm}} \end{pmatrix} = \begin{array}{c} \begin{matrix} g_{\mathrm{en}} & g_{\mathrm{fs}} & g_{\mathrm{mgts}} & g_{\mathrm{fm}} \end{matrix} \\ \begin{pmatrix} 1 & 0 & 0 & 0 \\ 0 & 1 & 0 & 0 \\ -1 & 0 & 1 & 1 \\ 0 & 0 & 0 & 1 \end{pmatrix} \end{array} \cdot \begin{pmatrix} g_{\mathrm{en}} \\ g_{\mathrm{fs}} \\ g_{\mathrm{mgts}} \\ g_{\mathrm{fm}} \end{pmatrix}$$

$$+ \begin{array}{c} \begin{matrix} W_{\text{en-fs}} & W_{\text{en-mgts}} & W_{\text{en-fm}} & W_{\text{fs-mgts}} & W_{\text{fs-fm}} & W_{\text{mgts-fm}} \end{matrix} \\ \begin{pmatrix} 0 & 0 & 0 & 0 & 0 & 0 \\ 0 & 0 & 0 & 0 & 0 & 0 \\ 0 & -1 & -1 & 0 & 0 & 1 \\ 0 & 0 & 0 & 0 & 0 & 0 \end{pmatrix} \end{array} \cdot \begin{pmatrix} W_{\text{en-fs}} \\ W_{\text{en-mgts}} \\ W_{\text{en-fm}} \\ W_{\text{fs-mgts}} \\ W_{\text{fs-fm}} \\ W_{\text{mgts-fm}} \end{pmatrix} \tag{15}$$

or

$$\begin{aligned} g'_{\mathrm{en}} &= g_{\mathrm{en}} \\ g'_{\mathrm{fs}} &= g_{\mathrm{fs}} \\ g'_{\mathrm{fets}} &= -g_{\mathrm{en}} + g_{\mathrm{mgts}} + g_{\mathrm{fm}} - W_{\text{en-mgts}} - W_{\text{en-fm}} \\ &\quad + W_{\text{mgts-fm}} \\ g'_{\mathrm{fm}} &= g_{\mathrm{fm}}. \end{aligned} \tag{16}$$

These results show that $\boldsymbol{W} \rightarrow \boldsymbol{W}'$ results in equivalences that are more or less complex linear combinations. Note, however, that W_{ij}, being the W for the ij binary, is not dependent on the choice of which other end-members are with ij in the two independent sets. In the $g \rightarrow g'$ results, g'_{fets} involves the (expected) linear combination of g's (reflecting the reaction fets = −en + mgts + fm) *and* a linear combination of W's.

Ca-amphibole

The second example concerns calcic clinoamphiboles in the system Na_2O-CaO-MgO-Al_2O_3-SiO_2-H_2O, with mixing restricted, for simplicity of argument and illustration, to the A site, the two M2 site, and the four Ti sites. Thus the thermodynamics may be written in terms of an arbitrary choice of three end-members chosen from tremolite, hornblende, tschermakite, edenite, and pargasite (Fig. 3). Al substitutes for Mg on the M2 sites and for Si on the T1 sites, and Na substitutes for vacancies on the A site. The composition matrix for an independent set of end-members involving tr [$Ca_2Mg_5Si_8O_{22}(OH)_2$], ts [$Ca_2Mg_3Al_4Si_6O_{22}(OH)_2$], and pa [$NaCa_2Mg_4Al_3Si_6O_{22}(OH)_2$] is

$$\boldsymbol{C} = \begin{array}{c} \\ \mathrm{tr} \\ \mathrm{ts} \\ \mathrm{pa} \end{array} \begin{array}{c} \begin{matrix} n^{\mathrm{A}}_{\mathrm{V}} & n^{\mathrm{A}}_{\mathrm{Na}} & n^{\mathrm{M2}}_{\mathrm{Mg}} & n^{\mathrm{M2}}_{\mathrm{Al}} & n^{\mathrm{T1}}_{\mathrm{Al}} & n^{\mathrm{T1}}_{\mathrm{Si}} \end{matrix} \\ \begin{pmatrix} 1 & 0 & 2 & 0 & 0 & 4 \\ 1 & 0 & 0 & 2 & 2 & 2 \\ 0 & 1 & 1 & 1 & 2 & 2 \end{pmatrix} \end{array} \tag{17}$$

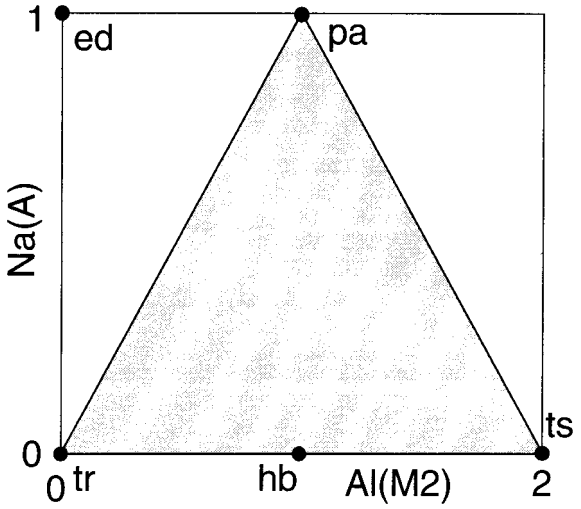

FIGURE 3. Compositions of amphibole end-members (tr, hb, ts, ed, and pa) in the NCMASH system. The shaded triangle is one possible independent set (tr-ts-pa) of end-members. The thermodynamics of an alternative choice of independent set (tr-ts-ed) is discussed in the text.

Taking a new independent set as tr, ts, and ed [$NaCa_2Mg_5AlSi_7O_{22}(OH)_2$], the composition matrix becomes

$$\boldsymbol{C}' = \begin{array}{c} \\ \text{tr} \\ \text{ts} \\ \text{ed} \end{array} \begin{array}{c} \begin{array}{cccccc} n^{\text{A}}_{\text{V}} & n^{\text{A}}_{\text{Na}} & n^{\text{M2}}_{\text{Mg}} & n^{\text{M2}}_{\text{Al}} & n^{\text{T1}}_{\text{Al}} & n^{\text{T1}}_{\text{Si}} \end{array} \\ \begin{pmatrix} 1 & 0 & 2 & 0 & 0 & 4 \\ 1 & 0 & 0 & 2 & 2 & 2 \\ 0 & 1 & 2 & 0 & 1 & 3 \end{pmatrix} \end{array} \tag{18}$$

and transforming the p's gives the new proportions

$$\begin{pmatrix} p'_{\text{tr}} \\ p'_{\text{ts}} \\ p'_{\text{ed}} \end{pmatrix} = \begin{pmatrix} p_{\text{tr}} - \frac{1}{2}p_{\text{pa}} \\ p_{\text{ts}} + \frac{1}{2}p_{\text{pa}} \\ p_{\text{pa}} \end{pmatrix} \tag{19}$$

The resulting equivalences for the interaction energies ($\boldsymbol{W}'$) and Gibbs energies ($\boldsymbol{g}'$) for the independent set involving tr, ts, and ed are

$$\begin{array}{c} \\ \begin{pmatrix} W'_{\text{tr-ts}} \\ W'_{\text{tr-ed}} \\ W'_{\text{ts-ed}} \end{pmatrix} \end{array} = \begin{array}{c} \begin{array}{ccc} W_{\text{tr-ts}} & W_{\text{tr-pa}} & W_{\text{ts-pa}} \end{array} \\ \begin{pmatrix} 1 & 0 & 0 \\ -\frac{1}{4} & \frac{1}{2} & \frac{1}{2} \\ \frac{3}{4} & -\frac{1}{2} & \frac{3}{2} \end{pmatrix} \end{array} \cdot \begin{pmatrix} W_{\text{tr-ts}} \\ W_{\text{tr-pa}} \\ W_{\text{ts-pa}} \end{pmatrix} \tag{20}$$

or

$$\begin{aligned} W'_{\text{tr-ts}} &= W_{\text{tr-ts}} \\ W'_{\text{tr-ed}} &= -\frac{1}{4}W_{\text{tr-ts}} + \frac{1}{2}W_{\text{tr-pa}} + \frac{1}{2}W_{\text{ts-pa}} \\ W'_{\text{ed-pa}} &= \frac{3}{4}W_{\text{tr-ts}} - \frac{1}{2}W_{\text{tr-pa}} + \frac{3}{2}W_{\text{ts-pa}} \end{aligned} \tag{21}$$

$$\begin{array}{c} \\ \begin{pmatrix} g'_{\text{tr}} \\ g'_{\text{ts}} \\ g'_{\text{ed}} \end{pmatrix} \end{array} = \begin{array}{c} \begin{array}{ccc} g_{\text{tr}} & g_{\text{ts}} & g_{\text{pa}} \end{array} \\ \begin{pmatrix} 1 & 0 & 0 \\ 0 & 1 & 0 \\ \frac{1}{2} & -\frac{1}{2} & 1 \end{pmatrix} \end{array} \cdot \begin{pmatrix} g_{\text{tr}} \\ g_{\text{ts}} \\ g_{\text{pa}} \end{pmatrix}$$

$$+ \begin{array}{c} \begin{array}{ccc} W_{\text{tr-ts}} & W_{\text{tr-pa}} & W_{\text{ts-pa}} \end{array} \\ \begin{pmatrix} 0 & 0 & 0 \\ 0 & 0 & 0 \\ -\frac{1}{4} & \frac{1}{2} & -\frac{1}{2} \end{pmatrix} \end{array} \cdot \begin{pmatrix} W_{\text{tr-ts}} \\ W_{\text{tr-pa}} \\ W_{\text{ts-pa}} \end{pmatrix} \tag{22}$$

or

$$\begin{aligned} g'_{\text{tr}} &= g_{\text{tr}} \\ g'_{\text{ts}} &= g_{\text{ts}} \\ g'_{\text{ed}} &= \frac{1}{2}g_{\text{tr}} - \frac{1}{2}g_{\text{ts}} + g_{\text{pa}} - \frac{1}{4}W_{\text{tr-ts}} + \frac{1}{2}W_{\text{tr-pa}} \\ &\quad - \frac{1}{2}W_{\text{ts-pa}} \end{aligned} \tag{23}$$

Thus the edenite Gibbs energy is a linear combination of the Gibbs energies of the other end-members and their interaction energies.

Biotite

The third example concerns biotite in the system K_2O-FeO-MgO-Al_2O_3-SiO_2-H_2O. An obvious choice of independent set involves phlogopite [phl; $KMg_2Mg(AlSi_3)O_{10}(OH)_2$], annite [ann; $KFe_2Fe(AlSi_3)O_{10}(OH)_2$], eastonite [eas; $KMg_2Al(Al_2Si_2)O_{10}(OH)_2$], and ordered biotite [obi; $KMg_2Fe(AlSi_3)O_{10}(OH)_2$]. So

$$\boldsymbol{C} = \begin{array}{c} \\ \text{phl} \\ \text{ann} \\ \text{eas} \\ \text{obi} \end{array} \begin{array}{c} \begin{array}{ccccccc} n^{\text{M2}}_{\text{Fe}} & n^{\text{M2}}_{\text{Mg}} & n^{\text{M1}}_{\text{Fe}} & n^{\text{M1}}_{\text{Mg}} & n^{\text{M1}}_{\text{Al}} & n^{\text{T}}_{\text{Al}} & n^{\text{T}}_{\text{Si}} \end{array} \\ \begin{pmatrix} 0 & 2 & 0 & 1 & 0 & 1 & 3 \\ 2 & 0 & 1 & 0 & 0 & 1 & 3 \\ 0 & 2 & 0 & 0 & 1 & 2 & 2 \\ 0 & 2 & 1 & 0 & 0 & 1 & 3 \end{pmatrix} \end{array} \tag{24}$$

and, for a new set, with siderophyllite [sid; $KFe_2Al(Al_2Si_2)O_{10}(OH)_2$] instead of eastonite, the composition matrix becomes

$$\boldsymbol{C}' = \begin{array}{c} \\ \text{phl} \\ \text{ann} \\ \text{sid} \\ \text{obi} \end{array} \begin{array}{c} \begin{array}{ccccccc} n^{\text{M2}}_{\text{Fe}} & n^{\text{M2}}_{\text{Mg}} & n^{\text{M1}}_{\text{Fe}} & n^{\text{M1}}_{\text{Mg}} & n^{\text{M1}}_{\text{Al}} & n^{\text{T}}_{\text{Al}} & n^{\text{T}}_{\text{Si}} \end{array} \\ \begin{pmatrix} 0 & 2 & 0 & 1 & 0 & 1 & 3 \\ 2 & 0 & 1 & 0 & 0 & 1 & 3 \\ 2 & 0 & 0 & 0 & 1 & 2 & 2 \\ 0 & 2 & 1 & 0 & 0 & 1 & 3 \end{pmatrix} \end{array} \tag{25}$$

and transforming the p's gives the new proportions as

$$\begin{pmatrix} p'_{\text{phl}} \\ p'_{\text{ann}} \\ p'_{\text{eas}} \\ p'_{\text{obi}} \end{pmatrix} = \begin{pmatrix} p_{\text{phl}} \\ p_{\text{ann}} - p_{\text{eas}} \\ p_{\text{eas}} \\ p_{\text{eas}} + p_{\text{obi}} \end{pmatrix} \quad (26)$$

with the W and g equivalences becoming

$$\begin{aligned} W'_{\text{phl-ann}} &= W_{\text{phl-ann}} \\ W'_{\text{phl-sid}} &= W_{\text{phl-ann}} + W_{\text{phl-eas}} - W_{\text{phl-obi}} - W_{\text{ann-eas}} \\ &\quad + W_{\text{ann-obi}} + W_{\text{eas-obi}} \\ W'_{\text{phl-obi}} &= W_{\text{phl-obi}} \\ W'_{\text{ann-sid}} &= W_{\text{eas-obi}} \\ W'_{\text{ann-obi}} &= W_{\text{ann-obi}} \\ W'_{\text{sid-obi}} &= -W_{\text{ann-eas}} + 2W_{\text{ann-obi}} + 2W_{\text{eas-obi}} \end{aligned} \quad (27)$$

and

$$\begin{aligned} g'_{\text{phi}} &= g_{\text{phi}} \\ g'_{\text{ann}} &= g_{\text{ann}} \\ g'_{\text{sid}} &= g_{\text{ann}} + g_{\text{eas}} - g_{\text{obi}} + W_{\text{ann-eas}} + W_{\text{ann-obi}} \\ &\quad - W_{\text{eas-obi}} \\ g'_{\text{obi}} &= g_{\text{obi}} \end{aligned} \quad (28)$$

It would be a difficult task to determine the binary mixing parameter $W_{\text{eas-obi}}$ in the original component set phl-ann-obi-eas, either by experiment or from natural data. However, the equivalences above show that $W_{\text{eas-obi}} = W_{\text{ann-sid}}$ and this could be determined, in principle, from experiments in the KFASH subsystem. Consideration of equivalences in different independent sets of end-members can help in the calibration of a complete set of mixing properties for a complex solid solution, as discussed further below.

Discussion

In the above section, the method of transforming the thermodynamics of minerals from one independent set to another was illustrated using examples from pyroxenes, amphiboles, and micas. In the following, general aspects of treating Fe-Mg phases are considered, then the thermodynamic descriptions of the minerals in the above examples are calibrated.

Simplification for Fe-Mg minerals

Fe-Mg site partitioning is a complication that arises in most Fe-Mg minerals. Although there are good site partitioning data for orthopyroxene in the system FeO-MgO-SiO_2, there are few data for biotite. In the literature, for phases such as biotite, it has been common practice to use equipartitioning of Fe and Mg, either implicitly or explicitly, in an attempt to simplify the thermodynamics. If this could be done, it would potentially decrease the number of end-members in the independent set by one (the ordered Fe-Mg end-member—for Fe-Mg partitioned between two sites) and thus decrease the number of W's needed by $n - 1$ (for an n end-member two-site phase); a useful reduction in the number of parameters that need to be calibrated. However, the partitioning must be considered an integral part of the thermodynamic description of the phase (whether it is with the symmetric formalism or not). The partitioning is the consequence of the equilibrium for an independent set of reactions between the end-members of the phase. For orthopyroxene, with Fe and Mg partitioned between Ml and M2, there is one reaction, for example en + fs = 2fm. Strict enforcement of equipartitioning not only denies the possibility of non-convergent ordering (as is seen in orthopyroxenes, orthoamphiboles, and cummingtonites) but also implies stringent relationships among the thermodynamic parameters. Thus, for a solid solution between ff (Fe_mFe_n) and mm (Mg_mMg_n) containing an ordered end-member fm (Fe_mMg_n), there are just two possibilities: (1) the trivial ideal case where all W terms and ΔH^0_R are zero; and (2) the non-ideal case in which there is only one independent interaction energy $W = w_{\text{ff-mm}}$. In the latter case, the other parameters are specified completely at any temperature above a disordering critical temperature T_c for the fm end-member:

$$\begin{aligned} \Delta H^0_R &= -RT_c\frac{(m+n)^2}{2} + \frac{mn}{m+n}W \\ w_{\text{fm-mm}} &= -RT_c\frac{(m+n)}{2} + \left(\frac{m}{m+n}\right)^2 W \\ w_{\text{fm-ff}} &= -RT_c\frac{(m+n)}{2} + \left(\frac{n}{m+n}\right)^2 W. \end{aligned}$$

These expressions for convergent ordering are derived from Equations 4–7 of Holland and Powell (1996b). For complete disorder, T_c must be below any geologically relevant temperature for mineral equilibration and, in the limiting case of T_c being zero, only the second term in each of the above expressions remains. Complete Fe-Mg ideality appears ruled out for most rock-forming silicates, and the restrictions imposed above suggest that equipartitioning is the rare, rather than the general, case.

This result has important ramifications for common Fe-Mg minerals, including pyroxenes, amphiboles, chlorite, and micas, for which consistent multicomponent mixing models must take Fe-Mg ordering explicitly into account. If simplifications of the Fe-Mg partitioning are needed, as they are in most minerals, then they have to be made with the full thermodynamic description as the starting point. There are various ways that such simplifications can be carried out. One way is to make an assumption about the similarity of Fe-Mg partitioning, at the thermodynamic level, in Fe-Mg-Al systems, Fe-Mg-Ca systems, and so on, in different minerals (effectively a corresponding-states approach). Another way is to look explicitly at the internal equilibria controlling Fe-Mg par-

titioning (as in the equilibrium relationship in orthopyroxene for reaction en + fs = 2fm mentioned above).

Using equivalences

To calibrate a simple FMAS orthopyroxene model requires obtaining values for the six independent interaction energies $W_{\text{en-fs}}$, $W_{\text{en-mgts}}$, $W_{\text{en-fm}}$, $W_{\text{fs-fm}}$, $W_{\text{fs-mgts}}$, and $W_{\text{mgts-fm}}$ as well as the enthalpy of the Fe-Mg-ordered pyroxene relative to en and fs. In the Al-free subsystem, there are sufficient experimental Fe-Mg partitioning experiments involving olivine-orthopyroxene (e.g., von Seckendorff and O'Neill 1993) and intracrystalline distribution of Fe-Mg (e.g., see review by Carpenter and Salje 1994) to determine reasonable values for $W_{\text{en-fs}}$ = 6.8 kJ/mol, and $W_{\text{fs-fm}}$ = 4.5 kJ/mol, together with a decrement of 6.95 kJ to be taken off the average of the enthalpies of en and fs to yield the enthalpy of fm (Holland and Powell 1996b).

In the Al-bearing system, fitting the Al contents of orthopyroxene coexisting with garnet and with spinel in the MAS system can be achieved with ideal mixing on the assumption that the Al-Si mixing on the tetrahedral sites is ignored (e.g., Danckwerth and Newton 1978; Perkins et al. 1981). Thus, the Tschermak substitution in MAS gives $W_{\text{en-mgts}}$ = 0. This assumption, first suggested by Wood and Banno (1973), works in this regard, but ultimately is not a satisfactory way of lowering the entropy of mixing, particularly in larger systems, for example, where Fe^{3+}-Al mixing is to be considered. The assumption that $W_{\text{en-mgts}}$ = 0 is made here because it is the simplest one for illustrating the principles.

Remaining to be found are $W_{\text{fs-mgts}}$ and $W_{\text{mgts-fm}}$. The approximation that $W_{\text{en-mgts}} \approx W_{\text{fs-fets}}$ is not only plausible but is required by the recent experiments of Aranovich and Berman (1997), the simple Wood-Banno entropy model is used. With this assumption, the equivalencies in Equation 14 yield $W_{\text{mgts-fm}} - W_{\text{fs-mgts}}$ = 2.2 in kJ/mol. One of these must be fixed to complete the thermodynamic description, with the Al solubility in orthopyroxene coexisting with garnet in the FAS system providing the experimental constraint (Aranovich and Berman 1997). The Gibbs energy of the fets end-member may be determined from Equation 16 and depends on the magnitude of $W_{\text{mgts-fm}}$ (given values for all the other terms in the expression). Only values close to $W_{\text{mgts-fm}}$ = 1.2 kJ/mol yield Gibbs energy for fets that can satisfy the experimental Al_2O_3 solubility of 1.1 wt% determined in the FAS system at 20 kbar and 1000 °C. The complete model is given by (in kJ/mol):

$$W_{\text{en-fs}} = 6.8 \qquad W_{\text{en-fm}} = 4.5$$
$$W_{\text{en-mgts}} = 0 \qquad W_{\text{fs-fm}} = 4.5$$
$$W_{\text{fs-mgts}} = -1.0 \qquad W_{\text{mgts-fm}} = 1.2$$
$$W_{\text{en-fets}} = 3.4 \qquad W_{\text{fets-fm}} = 0.$$
$$W_{\text{fs-fets}} = 0$$

The results of this simple model are tested against experimental data in Figure 4. The calculated Fe-Mg distribution between aluminous pyroxene and garnet at 20 kbar and 975 °C, and the absolute alumina content of such pyroxenes as a function of Fe/Mg ratio are in excellent agreement with the experimental findings of Perkins et al. (1981), Lee and Ganguly (1988), and Aranovich and Berman (1997). A more refined model should include a complete fit to the Aranovich and Berman data and should account for excess volumes of mixing on the en-mgts and

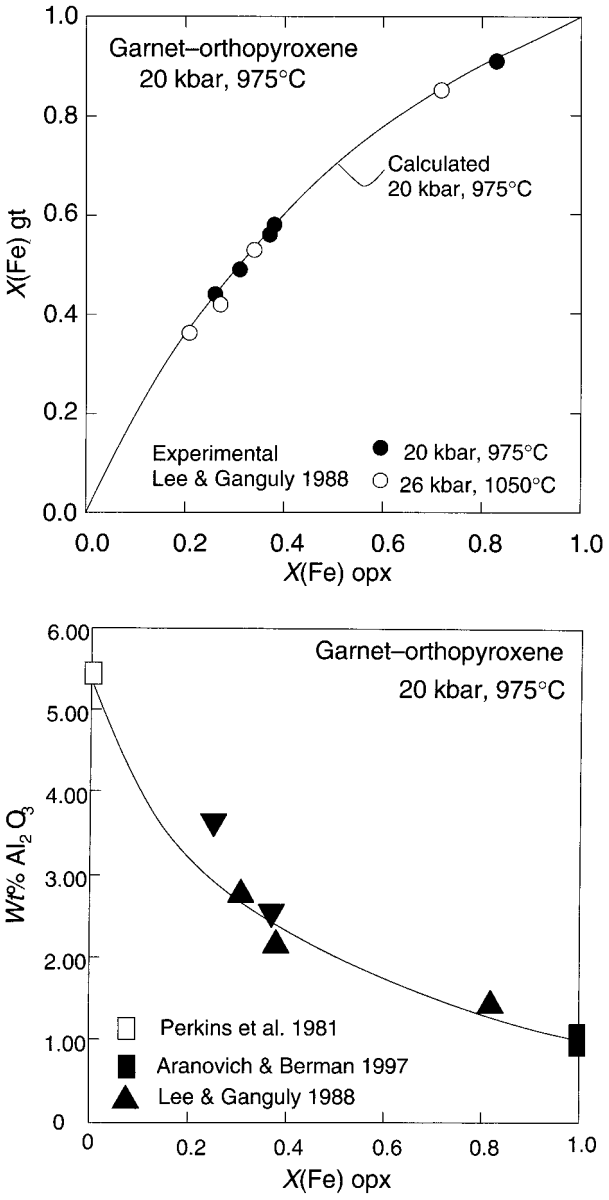

FIGURE 4. (**a**) Comparison of the calculated curve using the mixing model outlined in the text, and the experimental data of Lee and Ganguly (1988). (**b**) Comparison of the calculated curve using the mixing model outlined in the text, and the experimental data of Perkins et al. (1981), Lee and Ganguly (1988), and Aranovich and Berman (1997). All calculations used the program THERMOCALC.

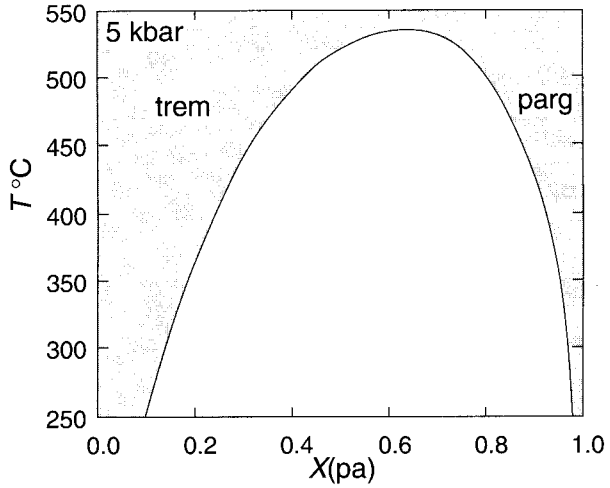

FIGURE 5. Calculated asymmetric solvus between tremolite and pargasite using program THERMOCALC and the mixing model outlined in the text.

fs-fets binary joins, together with a better model for tetrahedral site entropy reduction.

Considering the amphibole example, the simple tr-ts-pa system is critical for understanding the thermodynamics of aluminous amphiboles. In real situations, the system needs enlarging to include Na-Ca-Mg mixing on the M4 site as well as Fe-Mg substitutions, but the simpler situation above highlights the need for further experimental mixing data. The experiments of Jenkins (1994) on the tr-ts join provide a basis for recovery of the thermodynamic properties of tschermakite and the magnitude of $W_{\text{tr-ts}}$ (20 kJ/mol), whereas the experiments of Lykins and Jenkins (1993) and Sharma (1995) provide information on the tr-pa join. At present there are insufficient experimental data to determine this small subsystem of three independent end-members in a completely satisfactory manner. However, the experiments of Lykins and Jenkins (1993) fix the tremolite activity through the equilibrium 2tr + 2fo = 4di + 5en + $2H_2O$ to a value of 0.46 at 1.5 kbar and 880 °C, using the thermodynamic data for the mineral end-members from Holland and Powell (1998). The amphiboles lie close to the tr-pa join near $pa_{0.85}tr_{0.15}$ and so imply that $W_{\text{pa-tr}}$ is close to 44 kJ/mol. At 1.5 kbar and 880 °C, the tschermakite activity is fixed at a value of 0.0025 by the equilibrium 2ts = 4an + 2fo + en + $2H_2O$. Given the composition reported by Lykins and Jenkins, the ideal activity of ts is 0.0265 and therefore fixes the value of $RT\ln\gamma_{\text{ts}} = -22.6$ kJ/mol. With the values of $W_{\text{tr-ts}} = 20$ kJ/mol and $W_{\text{pa-tr}} = 44$ kJ/mol, the pa-ts interaction energy required to satisfy the ts activity is $W_{\text{pa-ts}} = -24$ kJ/mol. The experiments of Sharma (1995) lie at the tremolitic end of the pa-tr join and can be fitted well with a value of $W_{\text{pa-tr}} = 30$ kJ/mol, in contrast to the value of 44 kJ/mol determined from the pargasitic data of Lykins and Jenkins (1993). This difference in magnitude for $W_{\text{pa-tr}}$ deduced at each end of the series suggests more asymmetry in the tr-pa join than can be handled by the symmetric formalism. Although the amphiboles in both studies lie close to the tr-pa join, those in the experiments of Sharma are <15% pargasite whereas those of Lykins and Jenkins are >85% pargasite, which suggests a miscibility gap (cf. Oba 1980). The simple model above, with $W_{\text{pa-tr}} = 44$ kJ/mol, $W_{\text{tr-ts}} = 20$ kJ/mol, and $W_{\text{pa-ts}} = -24$ kJ/mol, generates an asymmetric miscibility gap closing at about 540 °C (at 5 kbar) with a crest near $pa_{0.65}tr_{0.35}$, (Fig. 5).

The ideal activity model used for these amphiboles is simple ideal mixing on the A and M2 sites, with half the entropy of T1 mixing. The site fractions are

$$X^{\text{A}}_{\text{Na}} = p_{\text{pa}}, \quad X^{\text{A}}_{\square} = 1 - p_{\text{pa}}, \quad X^{\text{M2}}_{\text{Al}} = \frac{2p_{\text{ts}} + p_{\text{pa}}}{2},$$

$$X^{\text{M2}}_{\text{Mg}} = \frac{2 - 2p_{\text{ts}} - p_{\text{pa}}}{2}, \quad X^{\text{T1}}_{\text{Al}} = \frac{p_{\text{ts}} + p_{\text{pa}}}{2} \quad \text{and}$$

$$X^{\text{T1}}_{\text{Si}} = \frac{2 - p_{\text{ts}} - p_{\text{pa}}}{2}$$

and lead to the following ideal mixing activities

$$a^{\text{ideal}}_{\text{tr}} = \frac{1}{16}(1 - p_{\text{pa}})(2 - 2p_{\text{ts}} - p_{\text{pa}})^2(2 - p_{\text{ts}} - p_{\text{pa}})^2$$

$$a^{\text{ideal}}_{\text{ts}} = \frac{1}{4}(1 - p_{\text{pa}})(2p_{\text{ts}} + p_{\text{pa}})^2(p_{\text{pa}} + p_{\text{ts}}) \times (2 - p_{\text{ts}} - p_{\text{pa}})$$

$$a^{\text{ideal}}_{\text{pa}} = p_{\text{pa}}(2p_{\text{ts}} + p_{\text{pa}})(2 - 2p_{\text{ts}} - p_{\text{pa}})(p_{\text{pa}} + p_{\text{ts}}) \times (2 - p_{\text{ts}} - p_{\text{pa}}).$$

The calibration of the biotite mixing model is more difficult because there are fewer experimental data. However, as discussed above, the thermodynamics must still start out in terms of the full complexity in terms of Fe-Mg partitioning between sites. The ideal activity model used for these biotites is simple ideal mixing on the Ml, M2, and T1 sites. The site fractions are

$$X^{\text{M1}}_{\text{Al}} = p_{\text{eas}}, \quad X^{\text{M1}}_{\text{Fe}} = 1 - p_{\text{eas}} - p_{\text{phl}},$$

$$X^{\text{M1}}_{\text{Mg}} = p_{\text{phl}}, \quad X^{\text{M2}}_{\text{Fe}} = p_{\text{ann}}, \quad X^{\text{T1}}_{\text{Al}} = \frac{1 + p_{\text{eas}}}{2} \quad \text{and}$$

$$X^{\text{T1}}_{\text{Si}} = \frac{1 - p_{\text{eas}}}{2}$$

and lead to the following ideal mixing activities:

$$a^{\text{ideal}}_{\text{phl}} = p_{\text{phl}}(1 - p_{\text{ann}})^2(1 - p_{\text{eas}})(1 + p_{\text{eas}})$$

$$a^{\text{ideal}}_{\text{ann}} = (1 - p_{\text{eas}} - p_{\text{phl}})p^2_{\text{ann}}(1 - p_{\text{eas}})(1 + p_{\text{eas}})$$

$$a^{\text{ideal}}_{\text{eas}} = \frac{1}{4}p_{\text{eas}}(1 - p_{\text{ann}})^2(1 + p_{\text{eas}})^2$$

$$a^{\text{ideal}}_{\text{obi}} = (1 - p_{\text{eas}} - p_{\text{phl}})(1 - p_{\text{ann}})^2(1 - p_{\text{eas}}) \times (1 + p_{\text{eas}}).$$

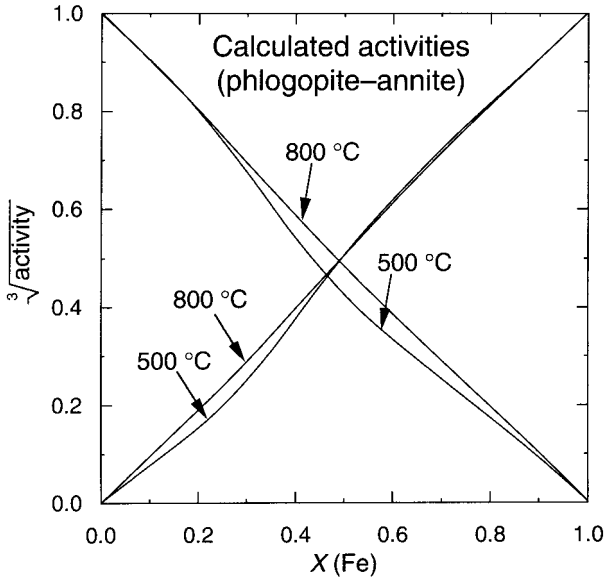

FIGURE 6. Calculated activities for phlogopite and annite in the binary Fe-Mg system without octahedral Al. The assumed Fe-Mg ordering leads to a pseudo-ideal solution at most temperatures.

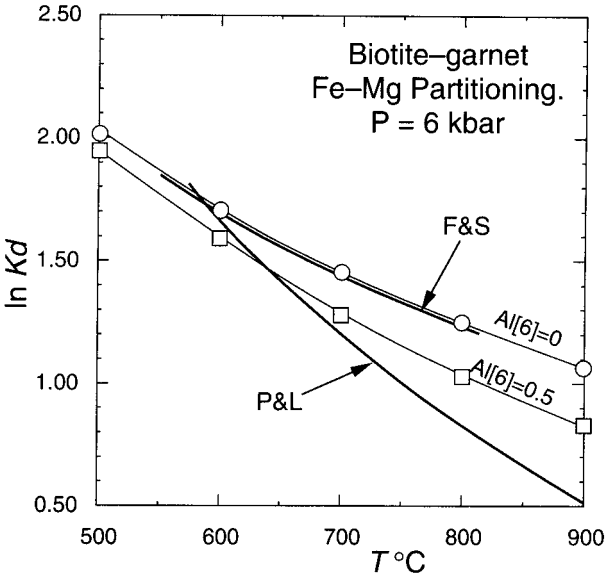

FIGURE 7. Calculated values (fine lines and symbols) for the distribution coefficient for Fe-Mg between garnet and biotite compared with the experimental studies (thicker lines). F&S = Ferry and Spear (1978), P&L = Perchuk and Lavrent'eva (1983). The calculated partitioning in the $^{[6]}$Al absent system is virtually identical to that of Ferry and Spear's study with phlogopite-annite biotites. The calculated partitioning for $^{[6]}$Al-bearing biotites is closer to the experimental study of Perchuk and Lavrent'eva (1983), who used natural biotites containing, $^{[6]}$Al, Ca, Mn, and Ti. A value of $W^{gt}_{Fe\text{-}Mg}$ = 2.5 kJ/mol (three-site basis) was assumed, and a composition of X^{gt}_{Fe} = 0.8 was fixed so as to be comparable with the study of Ferry and Spear, and all calculations were performed with the program THERMOCALC.

A way to start calibrating biotite is to assume that an average value for $w_{Fe\text{-}Mg}$ per octahedral site is 3 kJ/mol, giving $W_{phl\text{-}ann}$ = 9 kJ/mol, based on the molar volume relationship in Davies and Navrotsky (1983). If the equilibrium constant for the biotite internal equilibrium is taken to be independent of the Fe/Mg ratio, as in both orthopyroxenes and cummingtonites, this leads to the restriction $W_{ann\text{-}obi} = 3 + W_{phl\text{-}obi}$ (see the discussion in Holland and Powell 1996b). Taking 3 kJ/mol as a reasonable estimate for $W^{M1}_{FeMg} = W_{phl\text{-}obi}$ leads to $W_{ann\text{-}obi}$ = 6.0 kJ/mol. A corresponding-states argument is used to determine the enthalpy for the ordered end-member, obi, by assuming that the Fe-Mg ordering in biotites is similar to that observed in orthopyroxenes and cummingtonite-grunerites, in which a value for the order parameter Q is about 0.5 at the $Fe_{50}Mg_{50}$ composition at 1000 K. Following the approach for these other minerals (Holland and Powell 1996b), the enthalpy change for the reaction 2 phl + ann = 3 obi, using the W terms above, becomes −32.2 kJ/mol. These approximations allow calculation of activities in the phlogopite-annite system in which no octahedral Al occurs, and the results show that such biotites are predicted to be virtually ideal between 500 and 800 °C (Fig. 6). Such ideality in phlogopite-annite solid solutions has long been known (Wones 1972; Schulien 1975). To incorporate the Tschermak substitution into phlogopite, a value for $W_{phl\text{-}eas}$ is needed, and the calorimetric data of Circone and Navrotsky (1992) on the phl-eas join can be taken to imply $W_{phl\text{-}eas}$ is around 10 kJ/mol (Holland and Powell 1998). Using the plausible approximation (see the orthopyroxene example above) that $W_{phl\text{-}eas} \approx W_{ann\text{-}sid}$ = 10 kJ/mol and, from the equivalences noted earlier, that $W_{eas\text{-}obi} \approx W_{ann\text{-}sid}$, then a complete thermodynamic description just requires fixing a value for $W_{ann\text{-}eas}$. This last variable has a strong effect on the way $\ln K_D$ for Fe-Mg exchange between garnet and biotite varies with octahedral Al. A value of $W_{ann\text{-}eas} = -1$ kJ/mol allows agreement between calculated $\ln K_D$ and the experiments of Ferry and Spear (1978) for phlogopite-annite biotites, while reducing the discrepancy between calculated values and the experiments of Perchuk and Lavrent'eva (1983) on natural biotites (Fig. 7). Similar comparisons of experiments of Spear and of Perchuk and Lavrent'eva were made earlier by Aranovich et al. (1988). Thus the complete model for biotites becomes (in kJ/mol):

$$W_{phi\text{-}ann} = 9 \qquad W_{ann\text{-}obi} = 6$$
$$W_{phi\text{-}eas} = 10 \qquad W_{phi\text{-}obi} = 3$$
$$W_{ann\text{-}eas} = -1 \qquad W_{eas\text{-}obi} = 10.$$

Values for interactions involving siderophyllite may be derived from the list of equivalences given earlier. This description is not intended to be an optimal thermodynamic model of biotite mixing, but rather to show how the equivalences can be used to constrain the values of

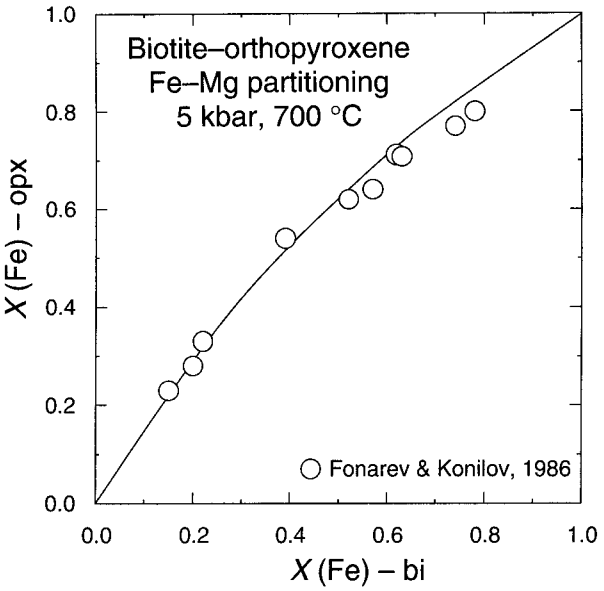

FIGURE 8. Calculated distribution of Fe and Mg between biotite and orthopyroxene at 700 °C and 5 kbar compared with the experimental data of Fonarev and Konilov (1986). All calculations used the program THERMOCALC.

the interaction energies, given some simple initial assumptions.

Calculation of the Fe-Mg partitioning between orthopyroxene and biotite should make a good test of the general reliability of the methods outlined here, as it makes use of the current model with both of the solid solutions involved. The partitioning at 5 kbar and 700 °C, calculated with the thermodynamic data of Holland and Powell (1998) and the models of this study, is compared with the experimental data of Fonarev and Konilov (1986) in Figure 8. With the exception of the most Fe-rich samples (which may have contained significant Fe^{3+}), the agreement is quite good. Thus, even with limited available information, it should be possible to generate activity models for other silicate solid solutions that incorporate reasonable assumptions about Fe-Mg ordering.

ACKNOWLEDGMENTS

We thank L. Aranovich and J. Ganguly for helpful comments and reviews.

REFERENCES CITED

Aranovich, L.Y. and Berman, R.G. (1997) A new garnet-orthopyroxene thermometer based on reversed Al_2O_3 solubility in FeO-Al_2O_3-SiO_2 orthopyroxene. American Mineralogist, 82, 345–353.

Aranovich, L.Y., Lavrent'eva, I.V., and Kosyakova, N.A. (1988) Biotite-garnet and biotite-orthopyroxene geothermometers—correction for the variable Al-content in biotite. Geokhimiya, 5, 668–676.

Benedict, M., Johnson, C.A., Soloman, E., and Rubin, L.C. (1945) Extractive and azeotropic distillation II. Separation of toluene from paraffins by azeotropic distillation with methanol. Transactions of the Institute of Chemical Engineering, 41, 371–392.

Carpenter, M.A. and Salje, E.K.H. (1994) Thermodynamics of non-convergent cation ordering in minerals, II: spinels and the orthopyroxene solid solution. American Mineralogist, 79, 1068–1083.

Circone, S. and Navrotsky, A. (1992) Substitution of $^{[6,4]}$Al in phlogopite: High temperature solution calorimetry, heat capacities, and thermodynamic properties of the phlogopite-eastonite join. American Mineralogist, 77, 1191–1205.

Danckwerth, P. and Newton, R.C. (1978) Experimental determination of the spinel peridotite to garnet peridotite reaction in the system MgO-Al_2O_3-SiO_2 in the range 900–1100 °C and Al_2O_3 isopleths of enstatite in the spinel field. Contributions to Mineralogy and Petrology, 66, 189–200.

Davies, P.K. and Navrotsky, A. (1983) Quantitative correlations of deviations from ideality in binary and pseudo-binary solid solutions. Journal of Solid State Chemistry, 46, 1–22.

Ferry, J.M and Spear, F.S. (1978) Experimental calibration of the partitioning of Fe and Mg between biotite and garnet. Contributions to Mineralogy and Petrology, 66, 113–117.

Fonarev, V.I. and Konliov, A.N. (1986) Experimental study of Fe-Mg distribution between biotite and orthopyroxene. Contributions to Mineralogy and Petrology, 93, 227–235.

Holland, T.J.B. and Powell, R. (1990) An internally-consistent thermodynamic dataset with uncertainties and correlations: the system Na_2O-K_2O-CaO-MgO-MnO-FeO-Fe_2O_3-Al_2O_3-SiO_2-TiO_2-C-H_2-O_2. Journal of Metamorphic Geology, 8, 89–124.

———(1996a) Thermodynamics of order-disorder in Minerals 1: symmetric formalism applied to minerals of fixed composition. American Mineralogist, 81, 1413–1424.

———(1996b) Thermodynamics of order-disorder in Minerals 2: symmetric formalism applied to solid solutions. American Mineralogist, 81, 1425–1437.

———(1998) An internally-consistent thermodynamic data set for phases of petrological interest. Journal of Metamorphic Geology, 16.

Jenkins, D.M. (1994) Experimental reversals of the aluminum content of tremolitic amphiboles in the system H_2O-CaO-MgO-Al_2O_3-SiO_2. American Journal of Science, 294, 593–620.

Lee, H.Y. and Ganguly, J. (1988) Equilibrium compositions of coexisting garnet and orthopyroxene: experimental determinations in the system FeO-MgO-Al_2O_3-SiO_2, and applications. Journal of Petrology, 29, 93–113.

Lykins, R.W. and Jenkins, D.M. (1993) Experimental determination of pargasite stability relations in the presence of orthopyroxene. Contributions to Mineralogy and Petrology, 112, 405–413.

Oba, T. (1980) Phase relations in the tremolite-pargasite join. Contributions to Mineralogy and Petrology, 71, 247–256.

Perchuk, L.L. and Lavrent'eva, I.V. (1983) Experimental investigation of exchange equilibria in the system cordierite-garnet-biotite. In S.K. Saxena, Ed., Kinetics and Equilibrium in Mineral Reactions, 199–240. Springer Verlag,

Perkins, D., III., Holland, T.J.B., and Newton, R.C. (1981) The Al_2O_3 contents of enstatite in equilibrium with garnet in the system MgO-Al_2O_3-SiO_2 at 15–40 kbar and 900°–1600°C. Contributions to Mineralogy and Petrology, 78, 99–109.

Powell, R. and Holland, T.J.B. (1993) On the formulation of simple mixing models for complex phases. American Mineralogist, 78, 1174–1180.

Schulien, S. (1975) Determination of the equilibrium constant and the enthalpy for the Mg^{2+}-Fe^{2+} exchange between biotite and a salt solution. Fortschritte der Mineralogie, 52, 133–139.

von Seckendorff, V. and O'Neill, H.St.C. (1993) An experimental study of Fe-Mg partitioning between olivine and orthopyroxene at 1173, 1273 and 1423 K and 1.6 GPa. Contributions to Mineralogy and Petrology, 113, 196–207.

Sharma, A. (1995) Experimentally derived thermochemical data for pargasite and reinvestigation of its stability with quartz in the system Na_2O-CaO-MgO-Al_2O_3-SiO_2-H_2O. Contributions to Mineralogy and Petrology, 125, 263–275.

Strang, G. (1988) Linear algebra and its applications. Harcourt Brace Jovanovich, 505p.

Wones, D.R. (1972) Stability of biotite: a reply. American Mineralogist, 57, 316–317.

Wood, B.J. and Banno, S. (1973) Garnet-orthopyroxene and orthopyroxene-clinopyroxene relationships in simple and complex systems. Contributions to Mineralogy and Petrology, 42, 109–124.

MANUSCRIPT RECEIVED OCTOBER 31, 1997
MANUSCRIPT ACCEPTED AUGUST 10, 1998
PAPER HANDLED BY JONATHAN F. STEBBINS

Appendix 1: Orthopyroxene example details

(a) Determining the relationships between p and y, x_1, and x_2

First the transpose of the composition matrix, $\boldsymbol{C}$, (Eq. 9), is augmented by a column representing each row of $\boldsymbol{C}^{\mathrm{T}}$ in terms of y, x_1, and x_2

$$\begin{pmatrix} 0 & 1 & 0 & 1 & x_2 \\ 1 & 0 & 1 & 0 & 1 - x_2 \\ 0 & 1 & 0 & 0 & x_1(1 - y) \\ 1 & 0 & 0 & 1 & (1 - x_1)(1 - y) \\ 0 & 0 & 1 & 0 & y \\ 0 & 0 & 1 & 0 & y \\ 2 & 2 & 1 & 2 & 2 - y \end{pmatrix}. \tag{29}$$

Next the nullspace of this matrix is determined (e.g., Strang 1988, p. 74–77). If there is just one row in the nullspace, it means that the number of end-members is correct. No rows means insufficient phases. More than one row means that there are reactions between the end-members, implying that the end-members do not constitute an independent set. The one row of the nullspace gives the correspondency between the p's and y, x_1, and x_2

$$\begin{pmatrix} p_{\mathrm{en}} \\ p_{\mathrm{fs}} \\ p_{\mathrm{mgts}} \\ p_{\mathrm{fm}} \end{pmatrix} = \begin{pmatrix} 1 - x_2 - y \\ x_1(1 - y) \\ y \\ -x_1 + x_2 + x_1 y \end{pmatrix}. \tag{30}$$

Such a calculation is straightforward to do with the symbolic computation facilities in *Mathematica*, using the built-in function, Nullspace: see Appendix Table 1. In a simple system like this, the number of independent end-members is easy to determine, for example via a figure like Figure 2; in complex systems it may be less straightforward. Ascertaining whether the number of end-members is determined correctly can be done as a part of a calculation to find the relationship between the proportions of the end-members in the independent set (p_{en}, p_{fs}, p_{mgts}, and p_{fm}) and the composition variables used to characterize the phase.

(b) Determining the transform matrix, A

Finding the transform matrix, $\boldsymbol{A}$, so that $\boldsymbol{C}' = \boldsymbol{A}^{\mathrm{T}}\boldsymbol{C}$, is most easily done using the nullspace, as in (a) above. First the transpose of $\boldsymbol{C}$ is augmented by the negative of a column of the transpose of $\boldsymbol{C}'$. For example, $\boldsymbol{C}^{\mathrm{T}}$ with the third column of $\boldsymbol{C}'^{\mathrm{T}}$, which will give the third column of $\boldsymbol{A}$ as

Appendix Table 1. Function, *p2x*, used to perform the calculation in part **a** of the Appendix for the orthopyroxene example

definition:

```
p2x[c:{{_?NumberQ...}...}, xy_List, name_List] :=
  Module[{ns, n},
    ns = NullSpace[Transpose[Join[c, {-xy}]]];
    n = Length[ns];
    Which[ n == 0, "insufficient end-members",
           n > 1, "too many end-members",
           True, Thread[name→Simplify[Drop[ns[[1]], -1]/ns[[1, -1]]]]//
                 ColumnForm ] ]
```

calling function:

```
p2x[c, {x2, (1 - x2),
        x1 (1 - y), (1 - x1) (1 - y), y,
        y, 2 - y}, name]
```

output:

```
en → 1 - x2 - y
fs → x1 (1 - y)
mgts → y
fm → -x1 + x2 + x1 y
```

$$\begin{pmatrix} 0 & 1 & 0 & 1 & -1 \\ 1 & 0 & 1 & 0 & 0 \\ 0 & 1 & 0 & 0 & 0 \\ 1 & 0 & 0 & 1 & 0 \\ 0 & 0 & 1 & 0 & -1 \\ 0 & 0 & 1 & 0 & -1 \\ 2 & 2 & 1 & 2 & -1 \end{pmatrix}. \tag{31}$$

The nullspace has one row that gives the third column of A as $(-1\ 0\ 1\ 1)^{\mathrm{T}}$. In this way $\boldsymbol{A}$ is built up giving

$$\boldsymbol{A} = \begin{pmatrix} 1 & 0 & -1 & 0 \\ 0 & 1 & 0 & 0 \\ 0 & 0 & 1 & 0 \\ 0 & 0 & 1 & 1 \end{pmatrix} \text{ with}$$

$$\boldsymbol{A}^{-1} = \begin{pmatrix} 1 & 0 & 1 & 0 \\ 0 & 1 & 0 & 0 \\ 0 & 0 & 1 & 0 \\ 0 & 0 & -1 & 1 \end{pmatrix}. \tag{32}$$

(c) Determining W' and g'.

With $\boldsymbol{A}$, the $\boldsymbol{W}$ equivalences can be established. First $\boldsymbol{Q} = \boldsymbol{A}^{\mathrm{T}}\boldsymbol{W}\boldsymbol{A}$, (Eq. 7), is formed

$$\boldsymbol{Q} = \begin{pmatrix} 0 & W_{\text{en-fs}} & W_{\text{en-fm}} + W_{\text{en-mgts}} & W_{\text{en-fm}} \\ 0 & 0 & W_{\text{fs-fm}} + W_{\text{fs-mgts}} & W_{\text{fs-fm}} \\ 0 & -W_{\text{en-fs}} & -W_{\text{en-fm}} - W_{\text{en-mgts}} + W_{\text{mgts-fm}} & -W_{\text{en-fm}} + W_{\text{mgts-fm}} \\ 0 & 0 & 0 & 0 \end{pmatrix}. \quad (33)$$

Noting that $\boldsymbol{Q}$ must have non-zero terms on and below the diagonal moved or converted in order for it to become $\boldsymbol{W}'$, first $\boldsymbol{Q}_1$ (part of $\boldsymbol{Q}$ below the diagonal) and $\boldsymbol{Q}_2$ (part of $\boldsymbol{Q}$ above the diagonal) are formed

$$\boldsymbol{Q}_1^{\mathrm{T}} = \begin{pmatrix} 0 & W_{\text{en-fs}} & W_{\text{en-fm}} + W_{\text{en-mgts}} & W_{\text{en-fm}} \\ 0 & 0 & W_{\text{fs-fm}} + W_{\text{fs-mgts}} & W_{\text{fs-fm}} \\ 0 & 0 & 0 & -W_{\text{en-fm}} + W_{\text{mgts-fm}} \\ 0 & 0 & 0 & 0 \end{pmatrix} \quad (34)$$

and

$$\boldsymbol{Q}_2 = \begin{pmatrix} 0 & 0 & 0 & 0 \\ 0 & 0 & -W_{\text{en-fs}} & 0 \\ 0 & 0 & 0 & 0 \\ 0 & 0 & 0 & 0 \end{pmatrix}. \quad (35)$$

These, as $\boldsymbol{Q}_1^{\mathrm{T}} + \boldsymbol{Q}_2$ contribute directly to $\boldsymbol{W}'$. This leaves the diagonal matrix, $\boldsymbol{Q}_3$, made up of the diagonal elements of $\boldsymbol{Q}$, to be handled.

The only non-zero element in $\boldsymbol{Q}_3$ is the third element, $W_{\text{en-fm}} + W_{\text{en-mgts}} - W_{\text{mgts-fm}}$, denoted by u in the following. So, from Equation 7:

$$\boldsymbol{p}'^{\mathrm{T}}\boldsymbol{Q}_3\boldsymbol{p}' = (p'_{\text{fets}})^2 u \quad (36)$$

Writing $(p'_{\text{fets}})^2$ as $p'_{\text{fets}}(1 - p'_{\text{phi}} - p'_{\text{ann}} - p'_{\text{fm}})$, then

$$\boldsymbol{p}'^{\mathrm{T}}\boldsymbol{Q}_3\boldsymbol{p}' = (p'_{\text{fets}} - p'_{\text{fets}}\,p'_{\text{phi}} - p'_{\text{fets}}\,p'_{\text{ann}} - p'_{\text{fets}}\,p'_{\text{fm}})u, \quad (37)$$

which, in the manner of (8), can be written as

$$\boldsymbol{p}'^{\mathrm{T}}\boldsymbol{Q}_3\boldsymbol{p}' = \boldsymbol{p}'^{\mathrm{T}}\boldsymbol{q} + \boldsymbol{p}'^{\mathrm{T}}\boldsymbol{Q}'_3\boldsymbol{p}' \quad (38)$$

in which

$$\boldsymbol{q} = \begin{pmatrix} 0 \\ 0 \\ u \\ 0 \end{pmatrix} \quad \text{and} \quad \boldsymbol{Q}'_3 = \begin{pmatrix} 0 & 0 & u & 0 \\ 0 & 0 & u & 0 \\ 0 & 0 & * & u \\ 0 & 0 & 0 & 0 \end{pmatrix}. \quad (39)$$

The element marked by an asterisk is zero; it is in the position of the non-zero element of Q_3. Note that the u is placed in the rows and columns above and to the right of the asterisk, corresponding to the $p'_{\text{phl}}\,p'_{\text{fets}}$, $p'_{\text{ann}}\,p'_{\text{fets}}$, and $p'_{\text{fets}}\,p'_{\text{fm}}$ terms. (The term $\boldsymbol{q}$ is included in the Gibbs energy equivalences below). Combining the $\boldsymbol{Q}$'s as in Equation 8 gives the required result for $\boldsymbol{W}'$

$$\boldsymbol{W}' = \begin{pmatrix} 0 & W_{\text{en-fs}} & 2W_{\text{en-fm}} + 2W_{\text{en-mgts}} - W_{\text{mgts-fm}} & W_{\text{en-fm}} \\ 0 & 0 & W_{\text{en-fm}} - W_{\text{en-fs}} + W_{\text{en-mgts}} + W_{\text{fs-fm}} + W_{\text{fs-mgts}} - W_{\text{mgts-fm}} & W_{\text{fs-fm}} \\ 0 & 0 & 0 & W_{\text{en-mgts}} \\ 0 & 0 & 0 & 0 \end{pmatrix}. \quad (40)$$

The required result for the Gibbs energies of the end-members in the new independent set, $\boldsymbol{g}'$, is just $\boldsymbol{A}^{\mathrm{T}}\boldsymbol{g}$ augmented with the term $\boldsymbol{q}$ left over from converting $\boldsymbol{Q}$ to $\boldsymbol{W}'$ above

$$\boldsymbol{g}' = \begin{pmatrix} g'_{\text{en}} \\ g'_{\text{fs}} \\ g'_{\text{fets}} \\ g'_{\text{fm}} \end{pmatrix} = \begin{pmatrix} 1 & 0 & 0 & 0 \\ 0 & 1 & 0 & 0 \\ -1 & 0 & 1 & 1 \\ 0 & 0 & 0 & 1 \end{pmatrix} \cdot \begin{pmatrix} g_{\text{en}} \\ g_{\text{fs}} \\ g_{\text{mgts}} \\ g_{\text{fm}} \end{pmatrix} + \begin{pmatrix} 0 \\ 0 \\ -W_{\text{en-fm}} - W_{\text{en-mgts}} + W_{\text{mgts-fm}} \\ 0 \end{pmatrix}. \quad (41)$$

Appendix 2: The symmetric formalism for the orthopyroxene example

Following the development in Powell and Holland (1993), the macroscopic interactions can be written in terms of the same-site and cross-site interactions. For en-fs-fm-mgts there are ${}^4\mathrm{C}_2 = 6$ macroscopic W's. The microscopic contributions come from three w's from same-site mixing on M1 ($w^{\text{M1}}_{\text{MgFe}}$, $w^{\text{M1}}_{\text{MgAl}}$ and $w^{\text{M1}}_{\text{FeAl}}$), one on M2 ($w^{\text{M2}}_{\text{MgFe}}$), and one on T ($w^{\text{T}}_{\text{AlSi}}$), and two w's from cross-site mixing between M1 and M2 ($w^{\text{M1M2}}_{\text{FeFeMgMg}}$ and $w^{\text{M1M2}}_{\text{AlFeMgMg}}$), two between M1 and T ($w^{\text{M1T}}_{\text{AlSiMgAl}}$ and $w^{\text{M1T}}_{\text{AlSiFeAl}}$), and one between M2 and T ($w^{\text{M2T}}_{\text{FeSiMgAl}}$), making a total of ten microscopic w's. The equivalences are:

$$W_{\text{en-fs}} = w^{\text{M1}}_{\text{MgFe}} + w^{\text{M2}}_{\text{MgFe}} + w^{\text{M1M2}}_{\text{FeFeMgMg}}$$

$$W_{\text{en-fm}} = w^{\text{M2}}_{\text{MgFe}}$$

$$W_{\text{en-mgts}} = \frac{1}{4}w^{\text{T}}_{\text{AlSi}} + w^{\text{M1}}_{\text{MgAl}} - \frac{1}{2}w^{\text{M1T}}_{\text{AlSiMgAl}}$$

$$W_{\text{fs-fm}} = w^{\text{M1}}_{\text{MgFe}}$$

$$W_{\text{fs-mgts}} = \frac{1}{4}w^{\text{T}}_{\text{AlSi}} + w^{\text{M1}}_{\text{FeAl}} + w^{\text{M2}}_{\text{MgFe}} - w^{\text{M1M2}}_{\text{AlFeFeMg}} - \frac{1}{2}w^{\text{M1T}}_{\text{AlSiFeAl}} + \frac{1}{2}w^{\text{M2T}}_{\text{FeSiMgAl}}$$

$$W_{\text{fm-mgts}} = \frac{1}{4}w^{\text{T}}_{\text{AlSi}} + w^{\text{M1}}_{\text{MgAl}} + w^{\text{M2}}_{\text{MgFe}} - w^{\text{M1M2}}_{\text{AlFeMgMg}} - \frac{1}{2}w^{\text{M1T}}_{\text{AlSiMgAl}} + \frac{1}{2}w^{\text{M2T}}_{\text{FeSiMgAl}}.$$

Observation of macroscopic properties allows the six macroscopic W's to be determined; the ten microscopic w's are only known in these linear combinations.

In the context of changing the independent set from en-fs-fm-mgts to en-fs-fm-fets (see text), the macroscopic W's new to this independent set are:

$$W_{\text{en-fets}} = \frac{1}{4}w^{\text{T}}_{\text{AlSi}} + \frac{1}{4}w^{\text{M1}}_{\text{MgAl}} + \frac{1}{2}w^{\text{M2}}_{\text{MgFe}} + w^{\text{M1M2}}_{\text{AlFeMgMg}} - \frac{1}{2}w^{\text{M1T}}_{\text{AlSiMgAl}} - \frac{1}{2}w^{\text{M2T}}_{\text{FeSiMgAl}}$$

$$W_{\text{fs-fets}} = \frac{1}{4}w^{\text{T}}_{\text{AlSi}} + w^{\text{M1}}_{\text{FeAl}} - \frac{1}{2}w^{\text{M1T}}_{\text{AlSiFeAl}}$$

$$W_{\text{fm-fets}} = \frac{1}{4}w^{\text{T}}_{\text{AlSi}} + w^{\text{M1}}_{\text{MgAl}} - \frac{1}{2}w^{\text{M1T}}_{\text{AlSiMgAl}}.$$

It can be seen directly that finding the equivalences between the macroscopic W's is a non-trivial task.